Basal body number scales with cell size in *Tetrahymena thermophila*

Lisa Mitchell
Departmental Honors Thesis
April 7, 2021

Thesis Advisor:
Dr. Chad Pearson (University of Colorado Anschutz, Department of Molecular and Developmental Biology)

Committee Members:
Dr. Jennifer Martin (Department of Molecular, Cellular, and Developmental Biology)
Dr. Pamela Harvey (Department of Molecular, Cellular, and Developmental Biology)
Dr. Alison Vigers (Department of Neuroscience)

University of Colorado Boulder
Department of Molecular, Cellular, and Developmental Biology
Spring 2021

Table of Contents

Abstract

The control of basal body (BB) and ciliary number is important to ensure normal cilia-dependent fluid flow in multi-ciliated cells. In the ciliate, *Tetrahymena thermophila* BBs are organized into rows at the cell cortex and nucleate cilia for cellular motility. Importantly, the number of BBs remains relatively constant in *Tetrahymena* cells (Nanney, 1971). How this homeostatic balance of BB frequency is controlled during each cell cycle remains poorly understood. The mutant, *big1-1*, that causes larger cells with more BBs was used to investigate how cells regulate BB number (Frankel, 2008). *Big1-1* mutant cells are longer and wider than wild type (WT) cells and possess supernumerary BBs. This suggests that BB assembly promiscuously increases in *big1-1* cells. To investigate how *big1-1* cells gain more BBs, we measured the rates of new BB duplication. Consistent with the increased number of BBs in *big1-1* cells, new BB duplication and assembly is elevated. Moreover, *big1-1* BBs mature more rapidly than WT BBs. This suggests that rapid BB maturation renders new BBs competent to assemble more BBs, thereby increasing rate of new BB assembly at each cell cycle. Elevated temperature exacerbates the *big1-1* BB amplification and corresponding cell size increase. Conversely, media starvation of *big1-1* cells restores BB number and cell size to nearly normal levels. Also, we observe that *big1-1* cells contain similar BB density throughout their ciliary rows. Instead, we show that *big1-1* accommodate their supernumerary BBs in extra ciliary rows that are formed through in a ciliary force-dependent mechanism. We find that the regulation of *Tetrahymena* BB number and cell size are coupled. The increase in cell size results from more BBs per ciliary row and an increase in the number of ciliary rows. Collectively, this suggests that *big1-1* mutant cells lengthen and widen to accommodate their supernumerary BBs and to maintain normal BB density. The counting and regulation of BB number in *Tetrahymena* is necessary for daughter cells to properly inherit sufficient BBs for cell motility. In summary, *Tetrahymena* BB number is tightly regulated thereby ensuring normal cell size.

Introduction

The regulation of centriole duplication is a fundamental event to eukaryotic life. Cancerous cells often present with extra centrioles, causing invasive behavior and aneuploidy, two distinct hallmarks of cancer (Ben-David & Amon, 2020; Hanahan & Weinberg, 2011). Too few centrioles causes atypical cell cycle regulation and disrupts the formation of cilia that are required for biological processes including development, mucosal clearance, and cerebrospinal fluid flow throughout the nervous system (Wang & Dynlacht, 2018). In order for eukaryotic cells to divide properly, the number of centrioles must be highly regulated. Similarly, in ciliates before they are able to divide, they must duplicate all existing basal bodies (BBs, synonymous with centrioles), doubling total BB number. This ensures that daughter cells have enough BBs to nucleate sufficient cilia for motility (Galati et al., 2016; Nanney et al., 1978). If ciliates do not produce enough BBs before duplication, this will result in a reductional division where the daughter cell does not inherit sufficient BBs. Conversely, if ciliates produce too many BBs before duplication, this results in a supernumerary division where the daughter cell inherits too many BBs. Both a reductional or supernumerary division reduce cell motility of the resultant cells. The mechanisms of how eukaryotic or ciliated cells count their number of centrioles/BBs to determine when they can undergo division is still poorly understood. Here, we used *Tetrahymena* as an ideal model organism to study centriole dysregulation at a fundamental level.

Tetrahymena are unicellular, ciliated eukaryotes that live in fresh water. These cells are between 30-50μm long and 15-25μm wide. *Tetrahymena* have been identified to be from the Stramenopile-Alveolate-Rhizarian Group (SAR) lineage (Ruehle et al., 2016). Although humans and *Tetrahymena* have large evolutionary gaps, this model organism has been shown to use many conserved eukaryotic processes (Briguglio & Turkewitz, 2014; Lynch et al., 1995). These studies have illuminated that *Tetrahymena* are extremely important model organisms when studying membrane trafficking, motor proteins, endomembrane network, cytoskeleton, and cilia dynamics (Briguglio & Turkewitz, 2014; Meehl et al., 2016; Pearson & Winey, 2010). Here, we used *Tetrahymena* cells to study BB dysregulation because *Tetrahymena* cells present with hundreds of BB per cell.

Tetrahymena cells contain two populations of BBs. One population forms the oral apparatus (OA) and the other BBs can be found lining the cell cortex. The BBs lining the cell cortex nucleate cilia. It is the hydrodynamic coupling of these cilia that allows *Tetrahymena* to move throughout their environment. BBs are arranged in a specific organizational pattern in *Tetrahymena* cells. Each BB consists of triplet microtubules that are arranged into a cylinder of nine symmetrical microtubules (Bayless et al., 2016). BBs are approximately 500-600 nm in length and 180-220 nm in diameter (Allen, 1969). The cortical BBs are arranged in longitudinal ciliary rows. Data has shown that each BB also contains three BB appendage structures: striated fibers (SFs), transverse microtubules (tMTs), and post-ciliary microtubules (pcMTs) (Allen, 1969). These appendage structures help preserve the delicate organization of BBs throughout the cell. SFs extend anteriorly from the BB and connect to the neighboring BB pcMT (Galati et al., 2014; Jerka-Dziadosz et al., 1995; Soh et al., 2019). Many connections are made between the BB appendage structures and cytoskeletal components of the cell cortex to ensure BBs do not move in response to forces created by the asymmetrical ciliary beating pattern observed in

Tetrahymena. (Burke et al., 2014; Galati et al., 2014; Herawati et al., 2016; Mahuzier et al., 2018; Siller et al., 2017; Yang et al., 2018).

The organization of BBs throughout the cell cortex is highly regulated and controlled. Data has shown that *Tetrahymena* cells are able to count their number of BBs per ciliary row and number of ciliary rows (Nanney, 1971). Additionally, these cells are able to adjust either the number of ciliary rows or number of BBs per ciliary row in order to achieve an ideal cortical organization (Nanney, 1971). New BB duplication and maturation occurs in a process that ensures this cortical organization remains the same. As a new BB is duplicated, it will mature and migrate anteriorly along the SF until it is eventually inserted into the cell cortex. As mentioned earlier, the regulated control of BB duplication is necessary to ensure *Tetrahymena* cells can divide properly.

In this thesis, we aimed to answer the following question; how do *Tetrahymena thermophila* cells count and regulate the number of BBs. In order to study this, we used a mutant strain of *Tetrahymena* called *big1-1* identified by Joseph Frankel (Frankel, 2008). *big1-1* is a single, recessive genetic lesion that causes too many BBs in *T. thermophila. big1-1* was created by a random mutagenesis screen and selected due to its distinct phenotype (Frankel, 2008). The excessive numbers of BBs that these cells possess allow us to study increased BB dysregulation. Here, we investigate how *big1-1 Tetrahymena* cells organize these excessive BBs. We show that as cells increase their size, their total BB number also increases. We also show that there is more BB duplication events in *big1-1* cells. Additionally, *big1-1* BBs mature faster, which we hypothesize leads to accelerated BB duplication due to the presence of excess competent mature BBs. In *big1-1* cells we also observe more ciliary rows, which we show is due to new ciliary row formation which occurs through a ciliary force dependent mechanism. In summary, we find that *Tetrahymena* BB number is tightly regulated thereby ensuring normal cell motility and cortical BB organization is highly controlled.

Materials and Methods

T. thermophila culture

All *T. thermophila* cells were grown in 2% SPP media (2% proteose peptone, 0.2% glucose, 0.1% yeast extract, and 0.0003% Fe-EDTA). Cells were grown to cycling conditions, which was determined by cells in mid-log phase (3.0×10^{-5} – 5.0×10^{-5} cells/mL). To find cell count, a Coulter Counter Z1 (Beckman Coulter) was used. To arrest cell cycle, cells were washed and grown in 10mM Tris-HCl, pH 7.4 for 24 h. Cells were passaged to keep cells at a mid-log concentration. When imaging, only non-dividing cells were analyzed, determined by presence of oral primordium. For experiments using the arrest and release protocol, cells were grown in 10mM Tris-HCl, pH 7.4 for 24 h. After this, they were transferred to SPP media, marking time 0h.

Tetrahymena strains

WT and *big1-1 T. thermophila* cells (B1868) that express mCherry-tagged SF proteins were created using the p4T2-1–mCherryLAP-POC1 construct (Pearson et al., 2009). In this study, BBs were visualized using the following BB proteins Poc1p, Sas6ap and Bld10p. To label microtubules, Beta-tubulin-2p was tagged using HaloTag® Technology and labelled via Janelia Fluor 549.

Increased/decreased ciliary force experiments

To elevate ciliary forces, cells were grown at high temperatures (37°C) for 24 h (Galati et al., 2014). Ciliary forces were reduced via NiCl2 treatment, which inhibit dynein-dependent ciliary beating by blocking membrane calcium channels and inhibiting dynein motors (Larsen & Satir, 1991).To address $NiCl_2$ cytotoxicity, the concentrations applied were determined empirically (Sigma-Aldrich). WT and *big1-1* cells were grown in 2mM and 1mM of $NiCl_2$, respectively.

BB, cilia, DNA labeling

To label BBs, cilia, and DNA, 7.5×10^5 cells were pelleted at 600 g in a 1.5-ml microcentrifuge tube and washed with 10mM Tris-HCl, pH 7.4 then PHEM, pH 6.9. Cells were fixed for 5 min with 1mL of 3.2%PFA/PHEM + 0.24% Triton X-100 (PHEM, 60 mM Pipes, 25 mM Hepes, 10 mM EGTA, and 2 mM $MgCl_2$, pH 6.9). Cells were then washed three times with 0.5% BSA/PBS. The primary antibody (rabbit anti-centrin [BB], 1:1000, mouse anti-α tubulin [611B], 1:1000) was added and left for 18 h at 4°C. The primary antibody was removed and cells were washed thrice with 0.5% BSA/PBS. Secondary antibody (mouse anti-rabbit Alexa Flour 547, 1:1000; rabbit anti-mouse Alexa Flour 488, 1:1000; (4′,6-diamidino-2-phenylindole), 1:1000) was added for 2 h at 4°C. Cells were washed three times with 0.5% BSA/PBS. Cells were mounted in Citaflour mounting media using #1.5 coverslips, and then sealed with clear nail polish. All antibodies were diluted in 0.5% BSA/PBS.

SF and MT labeling

To label SFs and MTs, 7.5×10^5 cells were pelleted at 600 g in a 1.5-ml microcentrifuge tube and washed with PHEM, pH 6.9. Cells were fixed for 5 min with 1mL of 3.2%PFA/PHEM + 0.24% Triton X-100 (PHEM, 60 mM Pipes, 25 mM Hepes, 10 mM EGTA, and 2 mM $MgCl_2$, pH 6.9) at 25°C. Fixative was remove and cells were pelleted again. Next, cells were

resuspended in ice cold 0.5% Triton X-100 (PHEM) for 10 minutes on ice at 4°C. Cells were washed three times using PHEM. Next, the cells were blocked in 0.5% BSA/PHEM for 1 h at 4°C. The primary antibody (mouse anti-SF [5D8], 1:500; rabbit anti-acetylated α-tubulin lysine 40 [D20G3; Cell Signaling Technology], 1:500) was added overnight at 4°C. Cells were washed three times with 0.5% BSA/PHEM. Next, the secondary antibody (goat anti-mouse Alexa Flour 488, 1:1000; goat anti-rabbit Alexa Flour 647, 1:1000; Invitrogen) was added for 2 h at 4°C. Cells were washed three times with 0.5% BSA/PHEM. Cells were mounted in Citaflour mounting media using #1.5 coverslips and sealed with nail polish. All antibodies were diluted in 0.5% BSA/PHEM.

Cell Tak and posted mounting

Experiments using a posted mounting used the following procedure. To promote cell adherence, coverslips were cleaned and treated with 3.5μm/cm^2 concentration of Cell Tak (Corning). The Cell Tak solution was prepared in 0.1M Sodium Bicarbonate with a pH between 6.5-8. Cell Tak was left on slides for 1 h and then washed twice with ddH_2O. Cells were placed onto coverslips and left for 18 h in 4°C. Excess cells were removed and mounted onto posted slides. Posts were created by a double layer droplet of nail polish in the corner of the coverslips. 100μL of Citaflour mounting media was placed in between the posts and the coverslips were inverted and placed on top. Slides were sealed with nail polish.

Light microscopy

Imaging experiments (Figure 2A, 2B, 3A, 3C, 3F, 4A; Supplemental Figure 4A) were performed with an inverted confocal microscope (Ti Eclipse) with a 100x Plan-Apochromat (NA1.43) objective lens (Nikon) using a Yokogawa CSU-X1 spinning disk module. All images were acquired with Slidebook with a z-step size of 200 nm at room temperature.
Additional imaging experiments (Figures 1A, 3H, 4B; Supplemental Figure 1A, 3A, 3B) were taken with another confocal microscope using an inverted microscope (Ti Eclipse) with a 100x Plan-Apochromat (NA 1.43) objective lens (Nikon) and a swept field confocal scan head with the 35μm slit mode (Prairie Technologies). Images were captured with a charge-coupled device camera(iXon X3; Andor Technology). These images were acquired with Nikon Elements with a z-step size of 300 nm at room temperature.

BB maturity assessment

In order to assess if a BB was considered a daughter or mother BB, the signal of the BB was recorded. To account for background signal, two additional measurements of signal were taken on regions directly adjacent to the signal of interest, and the average of these background signals was subtracted from the total signal. A nascent (dim) BB was considered to have a signal under 14,000 raw intensity units as calculated with FIJI and a mature (bright) BB was considered to have a signal over 14,000 raw intensity units as calculated with FIJI.

BB maturation analysis

To asses BB maturity, the length between the mother and daughter BB was acquired (interBB distance). Next, the signal was recorded from the mother and daughter BB, subtracting the average of two background signals on either side of the BB of interest. The ratio of mother/daughter signal was plotted against inter BB distance to asses for when BB maturation occurs.

BB ciliation analysis

To asses BB maturity, the length between the mother and daughter BB was acquired (interBB distance). Next, the presence of a cilium greater than 0.3μm in length on the daughter BB was recorded. A percentage of ciliated daughter BBs was calculated for various inter BB distances to determine when ciliation began.

Statistical analysis

All experimental datasets represent three biological replicates. The total number of cells and structures analyzed for each dataset is described in the figure legends. Student's t test was performed on normally distributed datasets. Tests for significance were two-tailed and unpaired. Error bars indicate SD. Statistical significance was set at P value <0.01.

Results

big1-1 cells are temperature sensitive mutants that exhibit enlarged cell size

Previous data has suggested that total BB number and cell size are coupled in WT cells. We wanted to see if we observed this mechanism in *big1-1* cells as well. In order to address this question, we grew WT and *big1-1* cells at a normal (30°C) and restrictive temperature (37°C) for 24 h after media starvation. We found that *big1-1* cells exhibit enlarged cell morphology (Figure 1A, 1B). We also found that the *big1-1* phenotype was exacerbated at elevated temperatures (Figure 1B). Additionally, at restrictive temperatures *big1-1* cells exhibit a variety of phenotypes with atypical cortical BB organization (Supplementary Figure 1A). Previous work in our lab has shown that dividing cells are larger and possess more BBs (Galati et al., 2016), so we next wanted to study this phenomenon in *big1-1* cells.

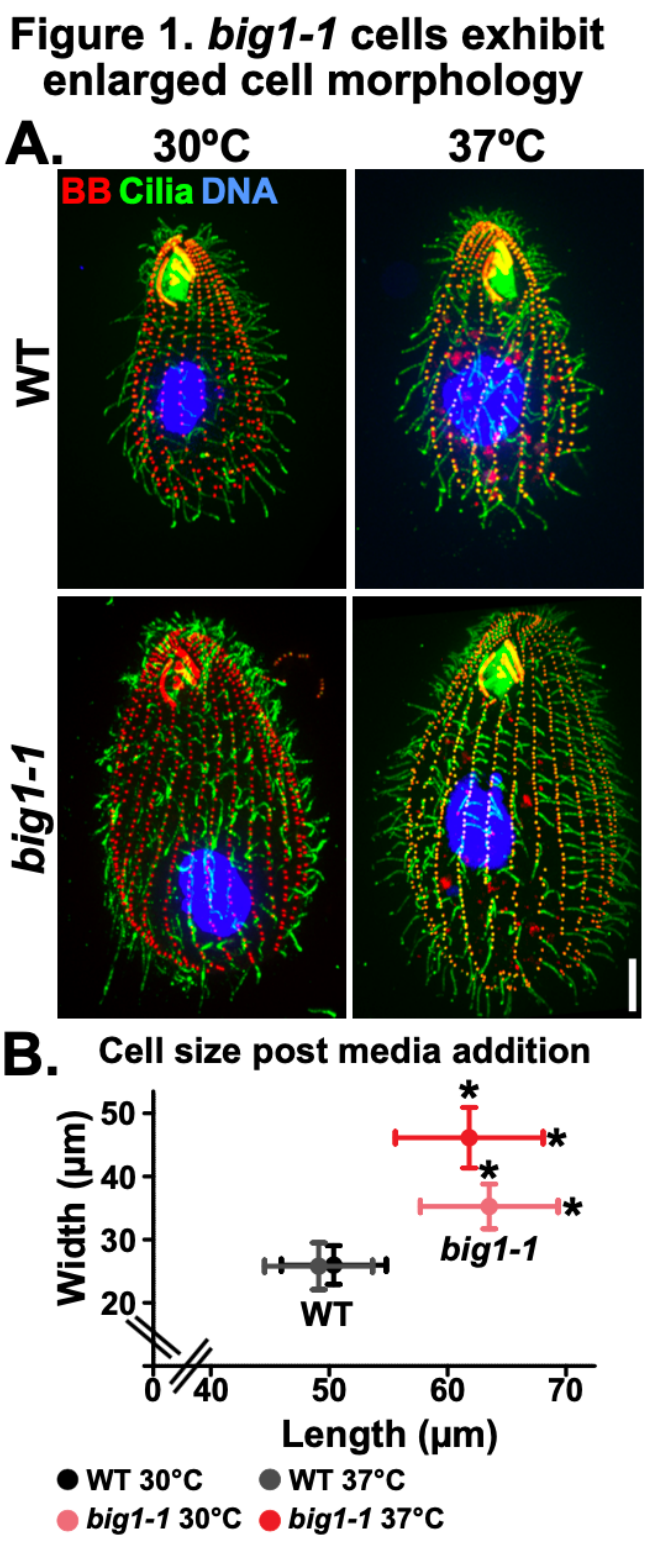

Figure 1. *big1-1* cells are temperature sensitive mutants that exhibit enlarged cell size. *big1-1* cells are generally larger and the increase in size is promoted by elevated temperature. **A.)** WT and *big1-1* cells increase slightly in length and width upon temperature increase. *big1-1* cells are dramatically larger that WT cells. Representative WT and *big1-1* cells at 30°C and 37°C. BBs (red, α-Cen1), cilia (green, DM1a), DNA (blue, Hoerscht33342). Scale bar, 10 µm. **B.)** Quantification of cycling WT and *big1-1* size grown at 30°C and 37°C. n = 32 cells. Students t-test. * P value <0.01. Mean ± SD.

big1-1 cells exhibit supernumerary BBs

After we observed that *big1-1* cells were larger, we wanted to see if *big1-1* cells also possessed more BBs. Due to the heterogeneity of *big1-1* cell size, we developed an assay to standardize cell morphology via a pre-starvation step. Next, we induced cycling conditions by the addition of media. To determine how BB number scales with cell size , we tracked the size and BB number in WT and *big1-1* cells over time (Figure 2A). We observed an increase in cell size in both WT and *big1-1* cells after media addition (Figure 2B). Additionally, we found that over time total BB number increased at the same time as cell size increased (Figure 2C). WT and *big1-1* cells were found to have significantly different number of BBs, with *big1-1* cells always containing more BBs (Figure 2C). Additionally, *big1-1* cells begin to gain more BBs sooner after media addition (Figure 2C). Since *big1-1* cells have more BBs, we next studied the placement of BBs.

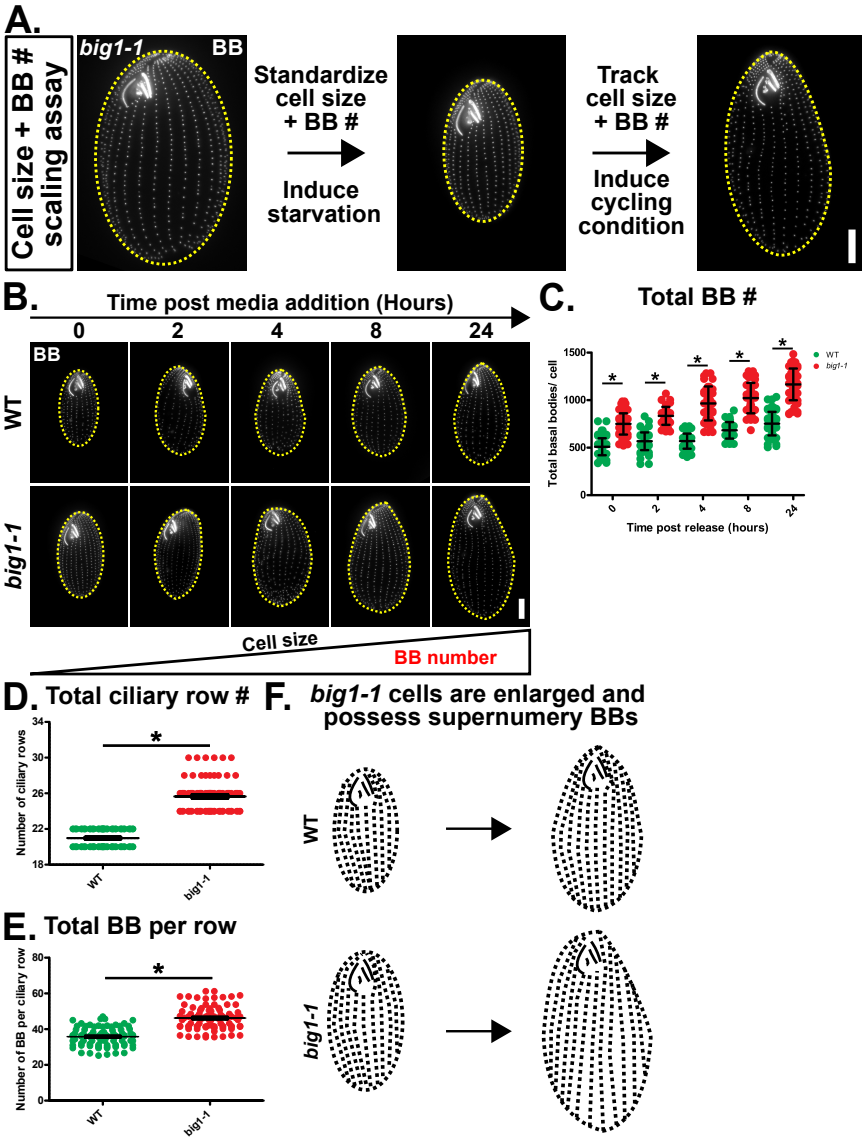

Figure 2. *big1-1* cells exhibit supernumerary BBs. *big1-1* cells possess more BBs in accordance with larger cell size. *big1-1* cells also have significantly more ciliary rows and BBs per ciliary row. **A.)** Assay developed in order to standardize *big1-1* cell size and total BB number. Images represent *big1-1* cells before and after standardization of cell size through starvation. All standardization was performed at 30°C. BBs (white, Poc1). Scale bar, 10 µm. **B.)** Growth assay of WT and *big1-1* cells. Images illustrate the time course of cycling *big1-1* cells at respective durations post media addition. BBs (white, Poc1). Scale bar, 10 µm. **C.)** Quantification of estimated total BB number in WT and *big1-1* cells. Students t-test. n = 36 cells. * P value <0.01. Mean ± SD. **D.)** Quantification of total ciliary rows in WT and *big1-1* cells 24 h post media addition. n = 36 cells. Students t-test. * denotes P value <0.01. Mean ± SD. **E.)** Quantification of total BB per ciliary row in WT and *big1-1* cells 24 h post media addition. n = 36 cells. Students t-test. * denotes P value <0.01. Mean ± SD. **F.)** Model representing *big1-1* enlarged cell size and supernumerary BBs.

In order to study BB placement in *big1-1* cells, we looked at the number of ciliary rows, ciliary row spacing, number of BBs per ciliary row and BB density in cells that were 24 h post media addition. From a BB spacing analysis, we observed that BB spacing is kept constant in *big1-1* cells, indicating constant BB density within a row (Supplementary Figure 2A). Similarly, from a ciliary row spacing analysis, we observed that ciliary row spacing is kept constant in *big1-1* cells, indicating constant ciliary row spacing within a cell (Supplementary Figure 2B). However, we found that *big1-1* cells contain a significantly higher number of ciliary rows per cell than WT cells do (Figure 2D). Also, *big1-1* cells contain more BB per ciliary row than WT cells do (Figure 2E). Thus, we hypothesized that because *big1-1* cells kept their BB density and ciliary row density constant, they were accounting for their supernumerary BBs through the lengthening of ciliary rows and the addition of new ciliary rows. We were able to conclude that *big1-1* cells contain supernumerary BBs compared to WT cells (Figure 2F). Additionally, *big1-1* cells possess more BB per ciliary row and ciliary rows while keeping BB density and ciliary row density consistent (Figure 2F). This suggests that even though *big1-1* cells produce more BBs, they are able to organize them conventionally. Since we saw excess BBs in *big1-1* cells, we next asked how *big1-1* cells produced these BBs.

BB duplication and maturation is accelerated in *big1-1* cells

Previous work has shown that *Tetrahymena* BBs can begin new BB duplication after they are mature and ciliated. We wanted to investigate how *big1-1* cells achieve supernumerary total BB number. In order to investigate how *big1-1* cells acquired excess BBs, we performed experiments using the BB protein Poc1. Poc1 is a BB component factor that incorporates as BBs mature. As more Poc1 is incorporated into the developing BB, the signal gets brighter. Using the endogenously labeled Poc1 strains of WT and *big1-1 Tetrahymena* cells revealed that *big1-1* cells contained more nascent BB synthesis (Figure 3A). We found that there were more events of immature BBs in *big1-1* cells compared to controls, indicating increased BB duplication (Figure 3A). We envisioned that *big1-1* cells could initiate BB duplication faster than WT cells in order to produce more BBs (Figure 3B). In order to address this hypothesis, we used Poc1 intensity of BBs in the medial region of the cell to investigate nascent BB assembly (Figure 3C). We found that WT cells had high levels of new BB assembly at 4 h and 6 h post media addition (Figure 3D). However, *big1-1* cells had high levels of new BB assembly at 2 h, 4 h, and 6 h post media addition (Figure 3D). Thus, we concluded that *big1-1* cells initiate nascent BB assembly faster than WT cells do and *big1-1* cells sustain this increased level of assembly for longer.

Next, we wanted to investigate *big1-1* BBs maturation. In order to study this, we performed a BB maturation assay that was previously established (Pearson et al., 2009). Here, we used inter BB distance as a readout for BB maturation (Figure 3E). We found that *big1-1* BBs mature faster than WT BBs using the Poc1 protein marker (Figure 3F). In order to ensure *big1-1* cells were maturing faster, we looked at this with two other BB proteins, Sas6a and Bld10. We found that *big1-1* BBs matured faster than controls with these BB proteins as well (Supplemental Figure 3A and 3B). In order for BBs to be functional, they need to be ciliated. Therefore to test the model that *big1-1* BBs were fully mature and functional, we created a BB ciliation assay (Figure 3G). Here, we used inter BB distance to assess for BB maturation using a BTU2-Halo microtubule marker (Figure 3G). We found that *big1-1* BBs begin ciliation at distances closer to the mother BBs when compared to control BBs (Figure 3H). Thus we concluded that *big1-1* BBs begin ciliation faster than WT BBs. Additionally, we concluded that *big1-1* BBs are fully mature due

to the fact that they are properly ciliated. Earlier, we noticed that *big1-1* cells contained extra ciliary rows, so we next set out to investigate how these rows were formed.

Figure 3. How do big1-1 cells generate more BBs?

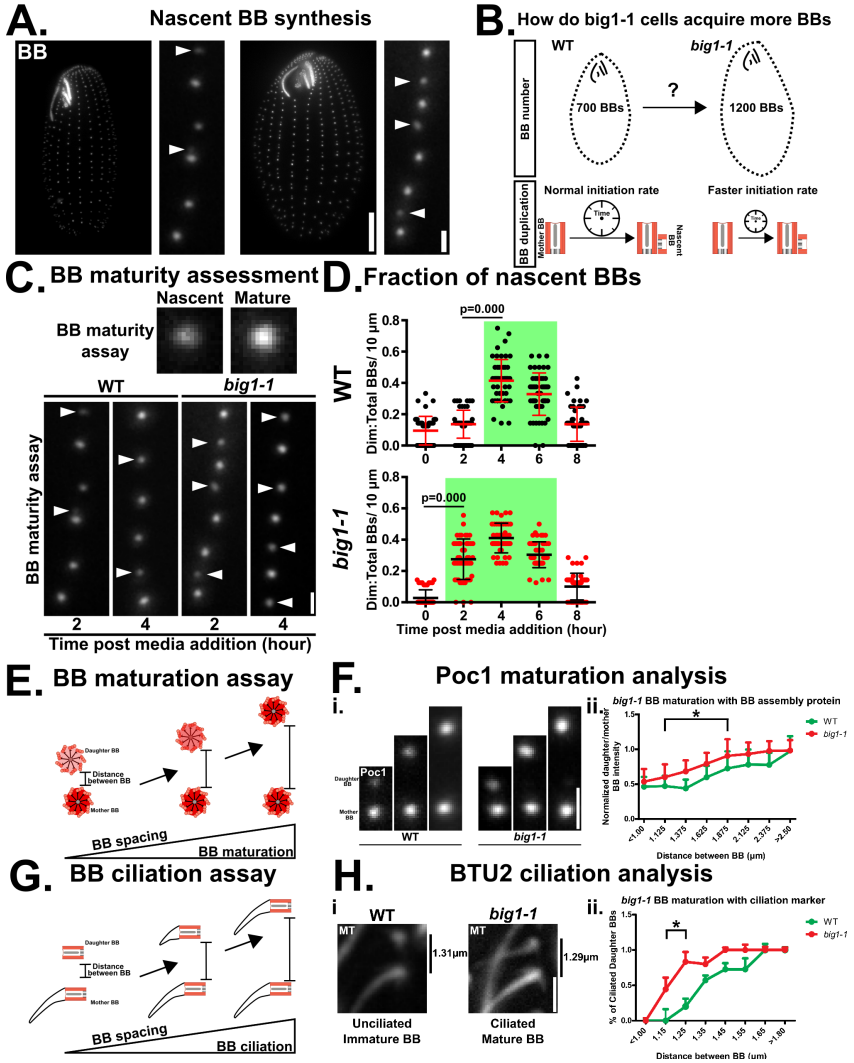

Figure 3. BB duplication and maturation is accelerated in *big1-1* cells. *big1-1* cells have more instances of BB duplication and *big1-1* BBs mature faster, which allows *big1-1* cells to attain supernumerary BBs. **A.)** Images depicting differences in nascent BB assembly between WT and *big1-1* cells. WT images (left) and *big1-1* images (right). BBs (white, Poc1). Scale bar, 10 µm. **B.)** Schematic representing a possible model of how *big1-1* cells acquire excess BBs. **C.)** BB maturity assay. BB duplication events were determined based on the fluorescence intensity of a mCherry tagged BB protein Poc1p. Dim Poc1p fluorescence intensity (white arrowheads) marks nascent BBs while bright Poc1p fluorescence intensity marks matured BBs. Images depict Poc1p labelled BBs in WT and *big1-1* cells at respective durations post release from starvation. Scale bar, 1 µm. **D.)** Proportion of nascent BB duplication events is initiated faster in *big1-1* cells and sustained longer. n = 38 cells. Students t-test. P value stated. Mean ± SD. **E.)** Assessment of BB maturity using BB marker protein. BB maturation was assessed by the fluorescence intensity mCherry tagged BB proteins, Poc1. During maturation, nascent BBs gain BB protein fluorescence intensity as they migrate anteriorly before insertion into the cell cortex. **F.)** *big1-1* BBs mature faster than WT BBs. (i.) Images depict that BBs of *big1-1* cells mature faster than WT cells as adjudged by Poc1 fluorescence intensity. Scale bar, 1 µm. (ii) Quantification of BB maturation of WT and *big1-1* cells. n = 30 cells, 10 pairs of BB per cell. Students t-test. * denotes P value <0.01. Mean ± SD. **G.)** Assessment of BB maturity using ciliation. BB ciliation was assessed by the endogenously labeled microtubule protein, BTU2. During maturation, nascent BBs begin to develop a cilium as they migrate anteriorly before insertion into the cell cortex. H.) (i) Images depict that BBs of big1-1 cells begin ciliation faster than WT cells as adjudges by BTU2 presence. Scale bar, 1 µm. (ii) Quantification of BB ciliation of WT and *big1-1* cells. n = 30 cells, 10 pairs of BB per cell. Students t-test. * denotes P value <0.01. Mean ± SD.

***big1-1* cells attain more ciliary rows via a ciliary force-dependent mechanism**

As we previously established that *big1-1* cells contain more BBs and more ciliary rows, we next set out to investigate how *big1-1* cells acquired new ciliary rows. When we were performing our cell cycle arrest and media addition experiments, we noticed short BB rows that were present in *big1-1* cells (Figure 4A). We hypothesized that these rows were the beginning of what would eventually become a complete ciliary row. In order to study the displaced BBs we saw, we categorized these events into three groups. The first group consisted of a BB gap where there was a larger inter BB distance than normal (Figure 4B). The second group consisted of BB that was displaced within a BB row (Figure 4B). Finally, we categorized the last group to contain partial BBs rows. After categorizing these events, we saw that after media was added to cells, there was a progression through these events (Supplemental Figure 4A). Additionally, there were more displaced BB events present at elevated ciliary force and in *big1-1* cells (Supplemental Figure 4A). Since we see more ciliary rows in *big1-1* cells, we started to think that these displaced BBs were the start of new ciliary row formation. Next, we began to hypothesize what could be causing these BBs to become displaced.

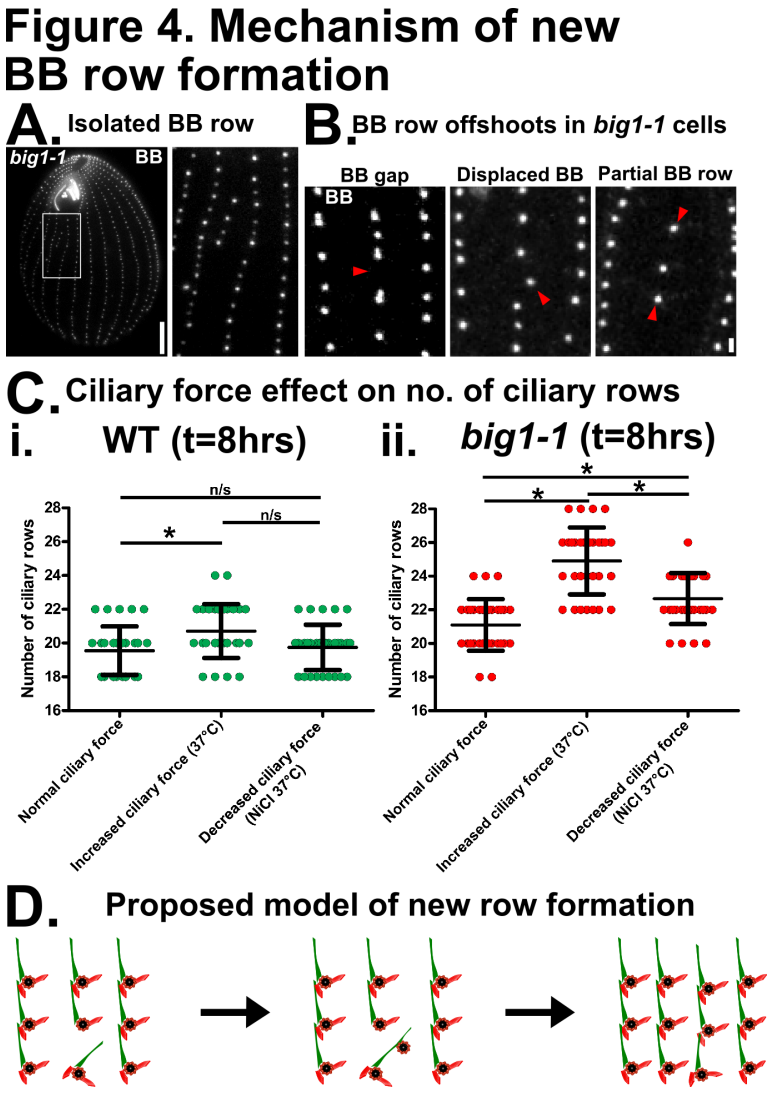

Figure 4. *big1-1* cells attain more ciliary rows via a ciliary force-dependent mechanism. New ciliary rows are formed through a ciliary force dependent mechanism in which asymmetrical ciliary forces cause BBs to be displaced and create a new row. **A.)** Image depicting incomplete BB rows observed in *big1-1* cells. BB (Poc1p), white. Scale bar, 10 µm. **B.)** Structured illumination microscopy (SIM) images illustrating the different BB row offshoot phenotypes. Group 1 shows slight BB veering (>30°). Group 2 shows BB veering (<30°). Group 3 shows independent but incomplete BB rows. BB (Poc1p), white. Scale bar, 1 µm. **C.)** Quantification of estimated ciliary row number in WT and *big1-1* cells at various levels of ciliary force. Elevated ciliary force (8 h at 37°C) correlated with more ciliary rows in both WT and *big1-1* cells. Conversely, reduced ciliary force ($NiCl_2$ induced inhibition of ciliary dynein motors (8 h at 37°C)) led to fewer ciliary rows. n = 32 cells. Students t-test. * denotes P value <0.01. Mean ± SD. **D.)** Schematic depicting proposed formation of new BB row. Arrowhead marks connection lost between SF and pcMT. BB, red; (SF), green; (pcMT), red.

Tetrahymena cells exhibit an asymmetric ciliary stroke, causing many different forces to be imposed upon BBs. Additionally, BBs nucleate cilia and anchor ciliary forces. Thus, we hypothesized that ciliary forces may affect the creation of new BB rows by displacing BBs out of BB rows. Once the displaced BB produces a daughter BB, the daughter BB would migrate anteriorly and create a new BB row. In order to test this model, we placed WT and *big1-1* cells in conditions of normal, increased, and decreased ciliary force. We found that in WT cells there was a significant increase in the number of ciliary rows between cells at normal and increased ciliary forces (Figure 4C). In *big1-1* cells, we also saw a significant increase in the number of ciliary rows between cells at normal and increased ciliary forces (Figure 4C). Additionally, we saw a significant decrease in the number of ciliary rows between *big1-1* cells at increased and decreased ciliary force conditions (Figure 4C). These findings led us to hypothesize that displaced BB are caused by ciliary forces. Once these displaced BBs duplicate more BBs, they will eventually form a full new ciliary row (Figure 4D). We have not been able to study this model in live imaging experiments, however that is something we plan to do in future studies. This data suggests that new ciliary rows in *T. thermophila* are formed in a mechanism that is caused by the asymmetrical ciliary beating pattern.

Discussion

Here, we set out to study the mechanisms of how *Tetrahymena* cells are able to count and organize their cortical BBs. This phenomenon was discovered in the 1970's but has remained a mystery since. In order to study BB dysregulation, we used a mutant strain of *Tetrahymena* called *big1-1*. We discovered that *big1-1* cells have increased cell size and supernumerary BBs. Through an assay we developed that was able to standardize cell size and BB number, we concluded that as *Tetrahymena* cells increase their total BB number, their cell size scales accordingly. We then went on to study *big1-1* cells and how they created and organized their supernumerary BBs.

We found that *big1-1* cells contain more events of BB duplication. This suggests that *big1-1* cells move through BB duplication faster than controls. Additionally, we found that *big1-1* BBs mature faster than control cells. Both of these mechanisms produce excess mature BBs which are then competent to produce additional nascent BB synthesis. We hypothesize that these processes are working together, not independent, in order to produce *big1-1* cells with supernumerary total BBs. It is important to note that due to faster BB maturation in *big1-1* cells, we believe we are under estimating our count of new BB duplication. Therefore, we hypothesize that the numbers of *big1-1* nascent BB duplication are even higher than what we have reported here.

After we determined how *big1-1* cells obtain their supernumerary BBs, we set out to study how they organize these BBs. We found that *big1-1* cells contain excessive ciliary rows and BBs per ciliary row. However, they also contain similar ciliary row spacing and BB density. This suggested to us that the cells elongate and widen in order to create longer ciliary rows and more ciliary rows. Previous work in the Pearson lab has shown that ciliary forces are transmitted through BBs and can cause shifting of BBs. As we observed displaced BBs, we hypothesized that they were being displaced due to forces created during asymmetrical ciliary beating. We tested this model by placing cells in conditions of elevated and decreased ciliary force and found that there were more ciliary rows in conditions of elevated ciliary force. This suggested to us that ciliary rows were formed in a ciliary force dependent mechanism. After observing different phenotypes of these displaced BBs and incomplete ciliary rows, we hypothesized that a connection between the posterior BB's SF and the anterior BB's pcMT is disrupted. Once this connection has been lost, the ciliary forces created during ciliary beating allow for the BB to begin to shift out of the ciliary row. We observed that all BB shifting was to the right of the existing row, which we think is due to the forces created during the ciliary waveform. Once these BBs have been displaced and undergo new BB duplication, the resultant daughter BB migrates anteriorly into the position of a new ciliary row. From here, a new ciliary row is started and BBs are produced towards the anterior end of the cell. In order to eventually form complete rows, we have envisioned a model to correct for incomplete BB rows. During cell division the cleavage furrow is in the medial region of the cell. Once the cell goes through division and splits at the medial region of the cell, the incomplete ciliary row becomes a complete ciliary row in the new daughter cell. This model is able to account for the fact that incomplete ciliary rows are rarely observed in cycling *Tetrahymena* cells. Moving forward, we hope to study this phenomenon using live imaging techniques and watch new ciliary row formation in real time.

The regulation of organelle duplication is an essential event of eukaryotic life. In this thesis, we aimed to study this process at a fundamental level using *Tetrahymena thermophila* cells, specifically looking at BB duplication. We found that size control is coupled to BB number regulation in *Tetrahymena*. As cells duplicate more BBs, total cell size increases. We also see this process happen when cells loose BBs, the total cell size decreases. These findings suggest that *Tetrahymena* can detect the number of BBs they possess, and increase or decrease their cell size accordingly. We hypothesize *Tetrahymena* cells count the number of BBs they possess by controlling the cortical network. Once extra BBs are found, the cortical network expands in order to accommodate the supernumerary BBs while keeping the BB density and ciliary row spacing consistent. Also, we hypothesize that additional BBs are added to existing ciliary rows to an arbitrary point, lengthening the cell. After the ciliary rows lengthen to a certain point, asymmetric ciliary forces cause connections within the cortical network to be lost and displaced BBs form. These displaced BBs undergo BB duplication and the daughter BBs create new ciliary rows, widening the cell. These findings build off David Nanney's work and show that *Tetrahymena* cells are able to adjust cell size in response to the number of BBs they possess. If BB duplication is dysregulated, this causes issues with division and the resultant cells have reduced cell motility. However, here we show that even cells with dysregulated BB duplication are able to control their cortical network. This shows that BB number regulation and BB deployment are independent processes. Understanding the conserved mechanism of counting and control of organelles and organelle duplication is essential to molecular biology.

Future Directions

This thesis set out to demonstrate how *Tetrahymena* cells change their BB numbers and resulting cortical organization. The conserved mechanisms of organelle duplication control are an active field of research. Since dysregulation of centrioles is present in many prevalent diseases, research into this field is promising. Live imaging techniques will give future researchers access to see centriole and BB dysregulation occurring in real time and subsequent changes in cortical organization. Moving forward with this project, we hope to identify the *big1-1* gene and finish developing a computational biology analysis pipeline.

In this project, we used a mutant strain of *Tetrahymena* that displayed increased numbers of BBs. *big1-1* is a single, recessive genetic lesion that causes increased numbers of centrioles in *T. thermophila*. In future projects, the identity of the *big1-1* gene and mutation will be identified. Next-Gen sequencing will be used to identify the *big1-1* gene and mutation. Subsequent experiments could localize the *Big1* protein to test whether it localizes to BBs. These experiments would reveal the functional role of the protein, possibly revealing if it was important for BB duplication or maturation. This study would identify novel regulators of BB duplication. Hopefully, this gene could then be a used as a new target for therapeutics aimed at treating diseases with centriole dysregulation.

Additionally, throughout the course of this project we have collaborated with Dr. Robert Murphy's lab at Carnegie Mellon University to create a computational biology analysis pipeline that can analyze the BB organization of *Tetrahymena* cells. In this collaboration, we are aiming to create an automated analysis of *Tetrahymena* cells to remove any inherent bias present in researchers. Currently, the automated analysis is able to detect BBs, either endogenously labeled or with antibody staining, and then sort these BBs into rows. This analysis also provides us with data about cell volume, row length, BB per row, BB density, ciliary row spacing, and intensity of BBs. We are also developing a code that is able to run a principle component analysis script between populations of cells. This program will be able to tell us what primary factors account for the variability we see between different populations and strains of *Tetrahymena* cells. This collaboration will revolutionize *Tetrahymena thermophila* cell biology by moving forward with a completely automated analysis.

Acknowledgments

I would first and foremost like to thank Dr. Chad Pearson. Not only did Dr. Pearson generously allow me to join the lab off a random email, he offered endless support. I was given his time, understanding, and support. Under his guidance, I have grown as a student immensely and could not be more grateful. My college career has been greatly enhanced by this experience.

Additionally, I would like to thank Adam Soh, my mentor and partner through this project. Adam pushed me to complete my best work and offered me nothing but patience when I was confused how to complete basic lab techniques. His imaging expertise and insightfulness allowed me to complete this project. Without his guidance, this thesis would not be possible.

I would also like to thank the additional members of the Pearson lab: Anthony Junker, Bailey McCurdy, Cayla Jewett, Alex Stemm-Wolf, Dr. Marisa Ruehle, Dr. Michelle Panzica, and Valerie Olsen. They offered a supportive environment, advice, and motivation. It was truly an honor to be part of the Pearson lab for the last few years.

I would like to thank the additional members of my honors committee, Dr. Martin, Dr. Harvey, and Dr. Vigers. I greatly appreciate all of your time, thoughts, and support throughout this process.

Finally, I would like to thank my family and friends for their support throughout the completion of my college degree and honors thesis. They were always willing to listen to me talk about data and experiments, even though they often did not understand.

This work was supported by the Undergraduate Research Opportunities Fund at the University of Colorado Boulder. I thank them for allowing me to complete this project.

References

1. Allen, R. D. (1969). The morphogenesis of basal bodies and accessory structures of the cortex of the ciliated protozoan tetrahymena pyriformis. *The Journal of Cell Biology*, *40*(3), 716–733.
2. Bayless, B. A., Galati, D. F., & Pearson, C. G. (2016). Tetrahymena basal bodies. *Cilia*, *5*. https://doi.org/10.1186/s13630-016-0022-8
3. Ben-David, U., & Amon, A. (2020). Context is everything: Aneuploidy in cancer. *Nature Reviews Genetics*, *21*(1), 44–62. https://doi.org/10.1038/s41576-019-0171-x
4. Briguglio, J. S., & Turkewitz, A. P. (2014). Tetrahymena thermophila: A divergent perspective on membrane traffic. *Journal of Experimental Zoology Part B: Molecular and Developmental Evolution*, *322*(7), 500–516. https://doi.org/10.1002/jez.b.22564
5. Burke, M. C., Li, F.-Q., Cyge, B., Arashiro, T., Brechbuhl, H. M., Chen, X., Siller, S. S., Weiss, M. A., O'Connell, C. B., Love, D., Westlake, C. J., Reynolds, S. D., Kuriyama, R., & Takemaru, K.-I. (2014). Chibby promotes ciliary vesicle formation and basal body docking during airway cell differentiation. *Journal of Cell Biology*, *207*(1), 123–137. https://doi.org/10.1083/jcb.201406140
6. Frankel, J. (2008). What do genic mutations tell us about the structural patterning of a complex single-celled organism? *Eukaryotic Cell*, *7*(10), 1617–1639. https://doi.org/10.1128/EC.00161-08
7. Galati, D. F., Abuin, D. S., Tauber, G. A., Pham, A. T., & Pearson, C. G. (2016). Automated image analysis reveals the dynamic 3-dimensional organization of multi-ciliary arrays. *Biology Open*, *5*(1), 20–31. https://doi.org/10.1242/bio.014951
8. Galati, D. F., Bonney, S., Kronenberg, Z., Clarissa, C., Yandell, M., Elde, N. C., Jerka-Dziadosz, M., Giddings, T. H., Frankel, J., & Pearson, C. G. (2014). DisAp-dependent striated fiber elongation is required to organize ciliary arrays. *Journal of Cell Biology*, *207*(6), 705–715. https://doi.org/10.1083/jcb.201409123
9. Hanahan, D., & Weinberg, R. A. (2011). Hallmarks of cancer: The next generation. *Cell*, *144*(5), 646–674. https://doi.org/10.1016/j.cell.2011.02.013
10. Herawati, E., Taniguchi, D., Kanoh, H., Tateishi, K., Ishihara, S., & Tsukita, S. (2016). Multiciliated cell basal bodies align in stereotypical patterns coordinated by the apical cytoskeleton. *Journal of Cell Biology*, *214*(5), 571–586. https://doi.org/10.1083/jcb.201601023
11. Jerka-Dziadosz, M., Jenkins, L. M., Nelsen, E. M., Williams, N. E., Jaeckel-Williams, R., & Frankel, J. (1995). Cellular polarity in ciliates: Persistence of global polarity in a disorganized mutant of tetrahymena thermophila that disrupts cytoskeletal organization. *Developmental Biology*, *169*(2), 644–661. https://doi.org/10.1006/dbio.1995.1176
12. Larsen, J., & Satir, P. (1991). Analysis of Ni(2+)-induced arrest of Paramecium axonemes. *Journal of Cell Science*, *99*(1), 33–40.
13. Lynch, T. J., Brickner, J., Nakano, K. J., & Orias, E. (1995). Genetic map of randomly amplified DNA polymorphisms closely linked to the mating type locus of Tetrahymena thermophila. *Genetics*, *141*(4), 1315–1325.
14. Mahuzier, A., Shihavuddin, A., Fournier, C., Lansade, P., Faucourt, M., Menezes, N., Meunier, A., Garfa-Traoré, M., Carlier, M.-F., Voituriez, R., Genovesio, A., Spassky, N., & Delgehyr, N. (2018). Ependymal cilia beating induces an actin network to protect

centrioles against shear stress. *Nature Communications*, *9*(1), 2279. https://doi.org/10.1038/s41467-018-04676-w

15. Meehl, J. B., Bayless, B. A., Giddings, T. H., Pearson, C. G., & Winey, M. (2016). Tetrahymena Poc1 ensures proper intertriplet microtubule linkages to maintain basal body integrity. *Molecular Biology of the Cell*, *27*(15), 2394–2403. https://doi.org/10.1091/mbc.E16-03-0165
16. Nanney, D. L. (1971). The constancy of cortical units in tetrahymena with varying numbers of ciliary rows. *Journal of Experimental Zoology*, *178*(2), 177–181. https://doi.org/10.1002/jez.1401780204
17. Nanney, D. L., Chen, S. S., & Meyer, E. B. (1978). Scalar constraints in Tetrahymena evolution. Quantitative basal body variations within and between species. *Journal of Cell Biology*, *79*(3), 727–736. https://doi.org/10.1083/jcb.79.3.727
18. Pearson, C. G., Osborn, D. P. S., Giddings, T. H., Beales, P. L., & Winey, M. (2009). Basal body stability and ciliogenesis requires the conserved component Poc1. *The Journal of Cell Biology*, *187*(6), 905–920. https://doi.org/10.1083/jcb.200908019
19. Pearson, C. G., & Winey, M. (2010). Plk4/SAK/ZYG-1 in the regulation of centriole duplication. *F1000 Biology Reports*, *2*, 58. https://doi.org/10.3410/B2-58
20. Ruehle, M. D., Orias, E., & Pearson, C. G. (2016). Tetrahymena as a Unicellular Model Eukaryote: Genetic and Genomic Tools. *Genetics*, *203*(2), 649–665. https://doi.org/10.1534/genetics.114.169748
21. Siller, S. S., Sharma, H., Li, S., Yang, J., Zhang, Y., Holtzman, M. J., Winuthayanon, W., Colognato, H., Holdener, B. C., Li, F.-Q., & Takemaru, K.-I. (2017). Conditional knockout mice for the distal appendage protein CEP164 reveal its essential roles in airway multiciliated cell differentiation. *PLOS Genetics*, *13*(12), e1007128. https://doi.org/10.1371/journal.pgen.1007128
22. Soh, A. W. J., van Dam, T. J. P., Stemm-Wolf, A. J., Pham, A. T., Morgan, G. P., O'Toole, E. T., & Pearson, C. G. (2019). Ciliary force-responsive striated fibers promote basal body connections and cortical interactions. *Journal of Cell Biology*, *219*(e201904091). https://doi.org/10.1083/jcb.201904091
23. Wang, L., & Dynlacht, B. D. (2018). The regulation of cilium assembly and disassembly in development and disease. *Development*, *145*(18). https://doi.org/10.1242/dev.151407
24. Yang, T. T., Chong, W. M., Wang, W.-J., Mazo, G., Tanos, B., Chen, Z., Tran, T. M. N., Chen, Y.-D., Weng, R. R., Huang, C.-E., Jane, W.-N., Tsou, M.-F. B., & Liao, J.-C. (2018). Super-resolution architecture of mammalian centriole distal appendages reveals distinct blade and matrix functional components. *Nature Communications*, *9*(1), 2023. https://doi.org/10.1038/s41467-018-04469-1

Supplemental Figures

Supplemental Figure 1.

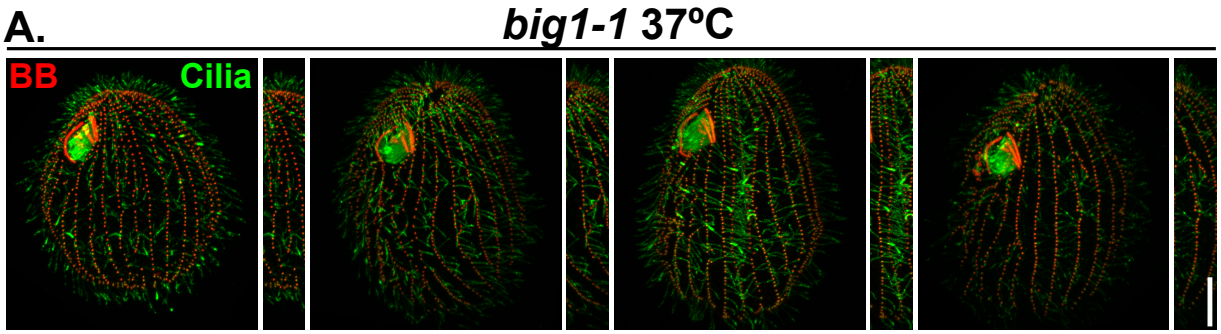

Supplemental Figure 1. *big1-1* cells present with a spectrum of phenotypes at restrictive temperatures. Elevated temperatures promote a variety of phenotypes in *big1-1* cells. **A.)** Upon temperature increase, *big1-1* cells exhibit ciliary row defects and cilia abnormalities. Insets represent various abnormalities. *big1-1* cells at 37°C. BBs (red, α-Cen1), cilia (green, DM1a), DNA (blue, Hoerscht33342). Scale bar, 10 μm.

Supplemental Figure 2.

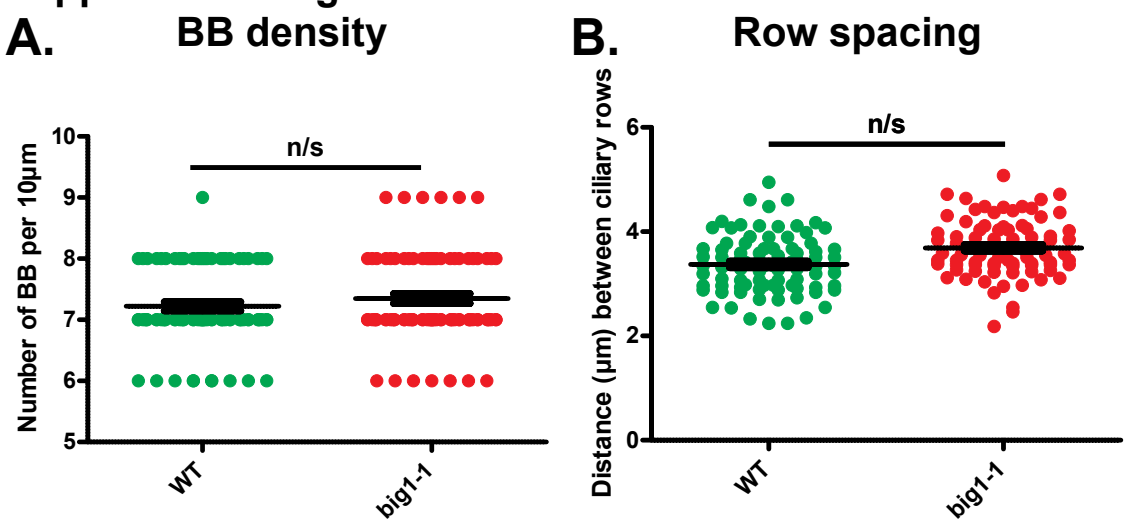

Supplemental Figure 2. WT and *big1-1* cells show similar BB cortical organization patterns. *big1-1* cells exhibit similar BB spacing within rows and spacing between rows as compared to WT cells, indicating similar cortical organization. **A.)** Quantification of BB density in WT and *big1-1* cells. BB density is measured in medial region of the cell. **B.)** Quantification of BB row spacing in WT and *big1-1* cells. BB row spacing is measured in medial region of the cell. All measurements were made at 24 h post release from starvation. n = 36 cells. Students t-test. * denotes P value <0.01. Mean ± SD.

Supplemental Figure 3.

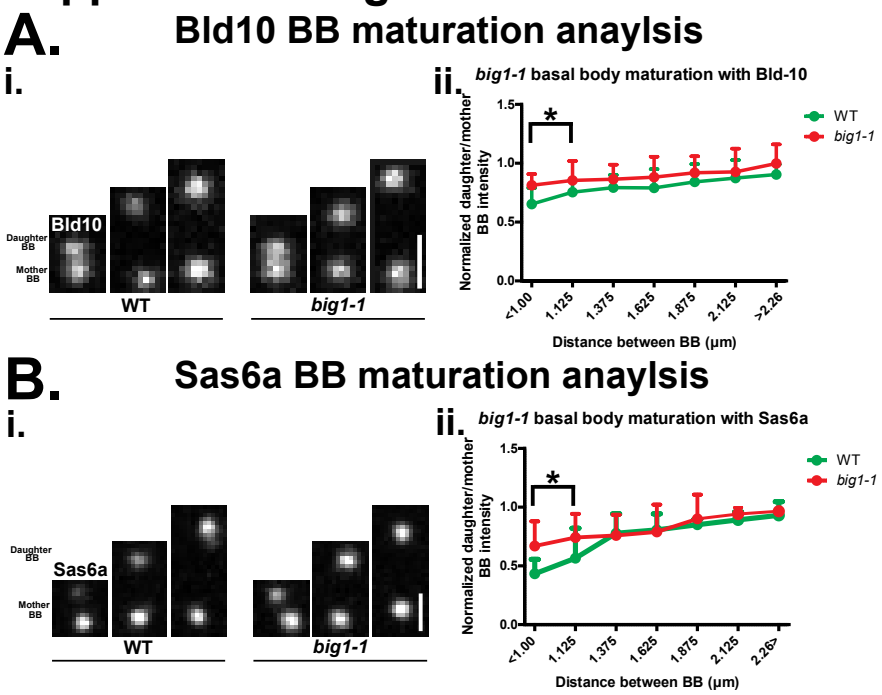

Supplemental Figure 3. *big1-1* BBs mature faster than WT BBs. Multiple endogenously labeled BB proteins show that *big1-1* cells mature faster. **A.)** (i.) Images depict that BBs of *big1-1* cells mature faster than WT cells as adjudged by Bld10 fluorescence intensity. (ii.) Quantification of BB maturation of WT and *big1-1* cells. n = 30 cells, 10 pairs of BB per cell. Students t-test. * denotes P value <0.01. Mean ± SD. Scale bar, 1 µm. **B.)** (i.) Images depict that BBs of *big1-1* cells mature faster than WT cells as adjudged by Sas6a fluorescence intensity. (ii.) Quantification of BB maturation of WT and *big1-1* cells. n = 30 cells, 10 pairs of BB per cell. Students t-test. * denotes P value <0.01. Mean ± SD. Scale bar, 1 µm.

Supplemental Figure 4.

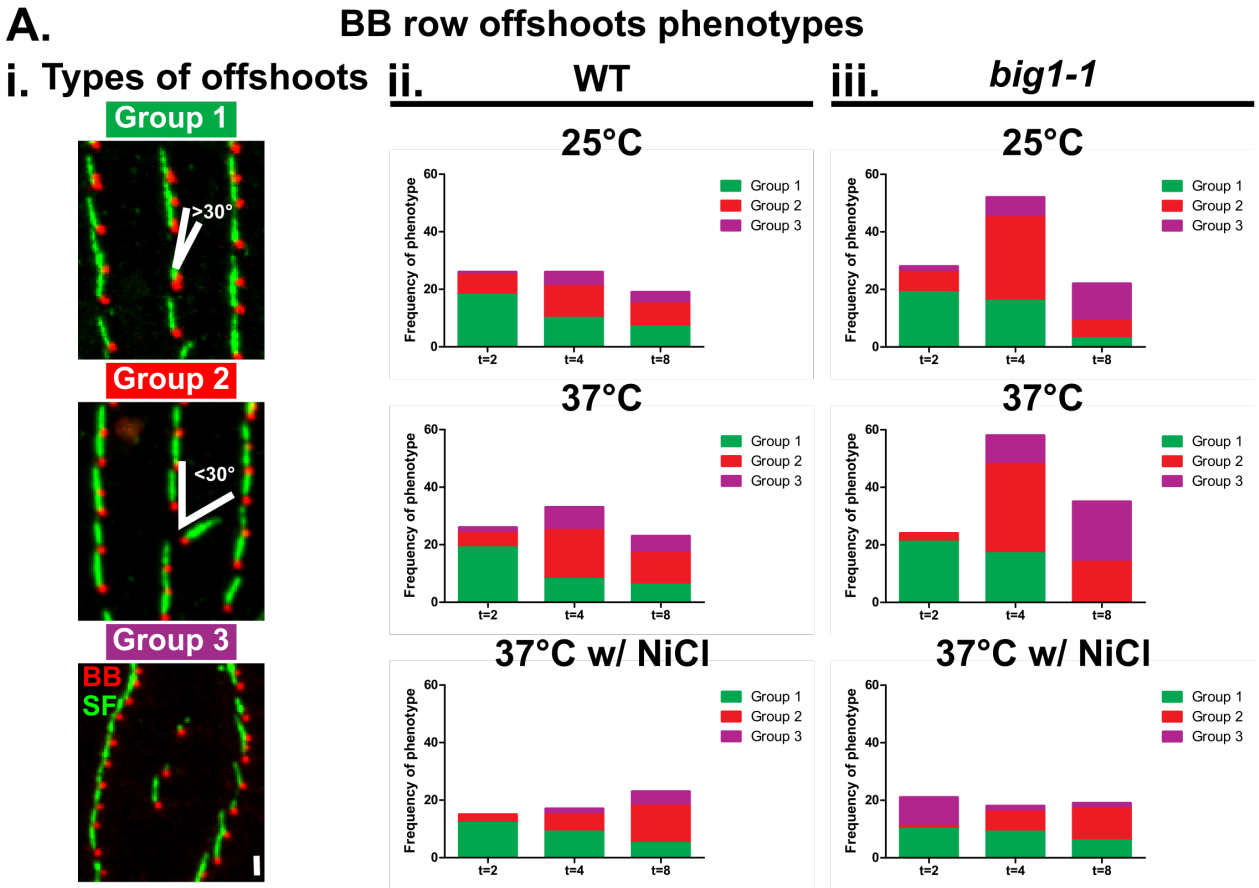

Supplemental Figure 4. New ciliary rows are formed through BB offshoots. As cells gain more ciliary rows (indicated by more time post media addition), they progress through the different BB offshoot phenotypes suggesting this is the mechanism for new row formation. Additionally, at reduced ciliary force conditions, there is a smaller frequency of all BB offshoot phenotypes in both WT and *big1-1* cells. *big1-1* cells exhibit a higher frequency of BB offshoot phenotypes. **A.)** (i.) Structured illumination microscopy (SIM) images illustrating the different BB row offshoot phenotypes. Group 1 shows slight BB veering (>30°). Group 2 shows BB veering (<30°). Group 3 shows independent but incomplete BB rows. BB (Poc1p), red; SF, green. Scale bar, 1 µm. (ii.) Quantification of frequency of BB row offshoot phenotypes in WT cells at various levels of ciliary force. Elevated ciliary force induces more BB row offshoot phenotypes while decreased ciliary force led to few BB row offshoot phenotypes. n = 30 cells. (iii.) Quantification of frequency of BB row offshoot phenotypes in *big1-1* cells at various levels of ciliary force. Elevated ciliary force induces more BB row offshoot phenotypes while decreased ciliary force led to few BB row offshoot phenotypes. Compared to WT cells, *big1-1* cells show higher levels of BB row offshoot phenotypes. n = 32 cells.